BIOLOGICALLY INSPIRED SLEEP ALGORITHM FOR INCREASED GENERALIZATION AND ADVERSARIAL ROBUSTNESS IN DEEP NEURAL NETWORKS

Anonymous authors
Paper under double-blind review

ABSTRACT

Current artificial neural networks (ANNs) can perform and excel at a variety of tasks ranging from image classification to spam detection through training on large datasets of labeled data. While the trained network usually performs well on similar testing data, certain inputs that differ even slightly from the training data may trigger unpredictable behavior. Due to this limitation, it is possible to generate inputs with very small designed perturbations that can result in misclassification. These adversarial attacks present a security risk to deployed ANNs and indicate a divergence between how ANNs and humans perform classification. Humans are robust at behaving in the presence of noise and are capable of correctly classifying objects that are occluded, blurred, or otherwise distorted. It has been hypothesized that sleep promotes generalization and improves robustness against noise in animals and humans. In this work, we utilize a biologically inspired sleep phase in ANNs and demonstrate the benefit of sleep on defending against adversarial attacks as well as increasing ANN classification robustness. We compare the sleep algorithm's performance on various robustness tasks with two previously proposed adversarial defenses, defensive distillation and fine-tuning. We report an increase in robustness after sleep to adversarial attacks as well as to general image distortions for three datasets: MNIST, CUB200, and a toy dataset. Overall, these results demonstrate the potential for biologically inspired solutions to solve existing problems in ANNs and guide the development of more robust, human-like ANNs.

1 INTRODUCTION

Although artificial neural networks (ANNs) have recently begun to rival human performance on various tasks, ranging from complex games (Silver et al. (2016)) to image classification (Krizhevsky et al. (2012)), they have been shown to underperform when the testing data differs in specific ways even by a small amount from the training data (Geirhos et al. (2018)). This lack of generalization presents two issues when ANNs are utilized in the real world. First, ANNs are often trained on curated datasets of images designed to best capture the image content, whereas in real-world scenarios, they may be tested on disturbed or noisy inputs, not observed during training. Second, ANNs are susceptible to adversarial attacks, or the deliberate creation of inputs designed to fool ANNs that may be imperceptibly different from correctly classified inputs (Szegedy et al. (2013)). These two issues limit the applicability of ANNs in the real world and present potential security risks when deployed.

There have been two main approaches for investigating ANN robustness: adversarial machine learning and training data manipulation (Ford et al. (2019)). Adversarial machine learning aims to develop novel attack methods which perturb the input minimally while changing the ANN's classification (Moosavi-Dezfooli et al. (2016); Carlini & Wagner (2017); Goodfellow et al. (2014); Athalye et al. (2017); Nguyen et al. (2015)) as well as to design defense mechanisms which prevent these attacks from affecting ANN behavior (Papernot et al. (2016b); Goodfellow et al. (2014); Huang et al. (2015), see Yuan et al. (2019) for review). Training data manipulation research typically examines the impact of changing the input distribution during testing and observing the effect on ANN performance. Geirhos et al. (2018) showed that ANNs trained on images with one type of distortion do

not perform as well when tested on other types of distortions, even if images with both distortions appear identical to the human eye. Likewise, ANNs trained on unperturbed images exhibit reduced performance when images in the test set are distorted, for example, through horizontal translations, blurring, or the addition of compression artifacts (Dodge & Karam (2016); Vasiljevic et al. (2016); Zhou et al. (2017)). Although it has been proposed that adversarial and manipulation robustness can be increased through various mechanisms during the training phase, such as fine-tuning, recent research has shown that these methods are mostly ineffective or their effectiveness is inconclusive (Geirhos et al. (2018); Uesato et al. (2018); Athalye et al. (2018)).

It has been hypothesized that in the mammalian brain sleep helps to create generalized representations of the input learned during the awake state (Stickgold & Walker (2013)). Sleep has been identified as being critical for memory consolidation - a process of converting recent memories into long-tern storage (Rasch & Born (2013)). During sleep, there is reactivation of neurons involved in previously learned activity (Stickgold (2005)) and this reactivation is likely to invoke the same spatio-temporal pattern as the pattern observed during training in the awake state (Wilson & McNaughton, 1994). Sleep reactivation, or replay, serves to strengthen synapses involved in a learned task through spike-timing dependent plasticity rules (STDP). Sleep, through STDP, can increase a subject's ability to form logical connections between memories and to generalize knowledge learned during the awake state (Payne et al. (2009)). In one study, subjects learned to find an exit to a maze in a virtual 3D environment starting at various positions. Subjects who were allowed to sleep exhibited a more complex understanding of the overall shape of the maze (Wamsley et al. (2010)). Using a biophysical model of cortical network, Gonzalez et al. (2019) and Wei et al. (2018) showed that sleep promotes reactivation and helps to create distinct representations for unique memories by devoting synapses to specific memory traces. This body of neuroscience work suggests that a sleep-like phase may be applied to ANNs to enable the networks to extract the gist of the training data and to rely less on the input statistics, which may be peculiar to the specifics of the training data and not the underlying distribution. Our hypothesis is that sleep could aid in reducing a neural network's susceptibility to adversarial attacks and to increase generalization performance by reducing the impact that imperceptible pixel changes can have on the task output.

In this new work, we propose a sleep-inspired algorithm to defend against adversarial attacks as well as to increase ANN robustness to noise. We utilize the notion of sleep from biology and apply an off-line unsupervised "sleep" phase to modify the parameters of a fully connected ANN. We demonstrate a number of performance improvements over existing defense algorithms, such as fine-tuning or adversarial retraining and defensive distillation, on both adversarial and noise robustness. The contributions are summarized below:

- We report positive results for four types of adversarial attacks tested on three different datasets (MNIST, CUB200, and a toy dataset) where following sleep the attack produces adversarial examples that are more distinct than the original input than before sleep.
- We illustrate that the sleep algorithm creates a more robust network whereby performance on noisy and blurred inputs is higher compared to a control or defensively distilled network and is more robust to the other distortions compared to ANNs that are fine-tuned on a single distortion.
- We analyze the impact of the sleep algorithm on task representation and demonstrate that the algorithm creates decision boundaries that more closely resemble the true classes, effectively extracting the gist of the data.

2 Adversarial Attacks and Distortions

Adversarial attacks aim to create minimal perturbations that, while imperceptible to the human eye, fool ANNs. These attacks range from white-box to black-box attacks, based on how much information they assume the attacker to possess about the network. White-box attacks assume that the attacker has access to the network architecture, training data and weights. These attacks can range from absolute information, such as gradient-based attacks which compute the gradient of the loss with respect to the input (Brendel et al. (2017)), to score-based attacks which only utilize predicted scores of the model. Black-box attacks, which assume no knowledge about the network, solely rely on the decision made in order to craft adversarial examples. Attacks can be targeted such that the attacker aims to create an adversarial example that the network predicts as a certain class or untargeted where the attacker's goal is simply to cause any kind of misclassification (Biggio & Roli (2018)).

In this work we consider four adversarial attacks ranging from white-box to black-box attacks. We assume that the attacker solely wants to cause a misclassification, with no respect to the output class. We present a brief description of each of the four attacks below (see Appendix for examples of images created by these attacks).

Fast Gradient Sign Method (FGSM). FGSM (Goodfellow et al. (2014)) computes the sign of the gradient of the loss function (J) with respect to the original input x using the weights θ of the network and the target labels y.

$$x' = x - \eta sign(\nabla_x J(\theta, x, y)).$$

This represents the direction to change each pixel in the original input in order to decrease the loss function. Based on the value of η, the corresponding perturbation to the original image can range from small to large. Thus, in this work we use the average of the smallest value of η needed to create an adversarial example x' (misclassified input) for each input in the testing set.

DeepFool. DeepFool (Moosavi-Dezfooli et al. (2016)) is an iterative method which approximates the nearest decision boundary to the input at time t and moves the input x_t in that direction to compute x_{t+1}. This process is repeated until a misclassification is produced or the runtime of the simulation is exceeded. For this attack, we measure the L2-norm between the original input x and the adversarial input x'. Thus, successful defenses should result in a high L2-norm for this algorithm.

Jacobian-based Saliency Map (JSMA). JSMA (Papernot et al. (2016a)) aims to craft adversarial examples that minimize the L0-norm of $x - x'$ by reducing the number of pixels that are altered. In summary, the algorithm computes the gradient, as done in FGSM but for all possible classes. These gradient values represent how changing each pixel contributes to the overall loss function, with large values indicating a significant effect on the loss. These values are used to create a saliency map, where each pixel's impact on the loss is modelled. The algorithm utilizes this saliency map to alter individual pixels, repeating the gradient and saliency map computation until an adversarial example is created. For this type of attack, we utilize the L2-norm to determine defense success.

Boundary Attack. The Boundary Attack (Brendel et al. (2017)) is a black-box attack which relies solely on the decision of the ANN to craft an adversarial example. Given an input x, a random input x'_0 is chosen such that $f(x) \neq f(x'_0)$, where $f(x)$ is the label produced by the ANN. In our work, x'_0 is chosen from a uniform distribution. The attack starts by moving x'_0 toward x until it reaches the point where $f(x) = f(x'_0)$, or the decision boundary in between $f(x)$ and $f(x'_0)$. From here, the attack consists of two steps: an orthogonal perturbation and a forward perturbation. During the orthogonal perturbation, random points along the hypersphere around $f(x'_t)$ are sampled. Those that are adversarial and closer to x than before are added to the queue for forward perturbation. During the forward perturbation, a small step is taken from x'_t to x as long as $f(x) \neq f(x'_t)$. This process is repeated until a convergence criterion is met. For this attack, we utilize the L2-norm to define defense success.

Distortions. Although not specifically designed to attack an ANN, distortions similarly corrupt ANN performance. In this work we consider two simple distortion techniques: blurring and Gaussian noise. For images, we perform 2-D Gaussian filtering with a blur kernel of varying standard deviation in order to blur the images. For all inputs, we add Gaussian noise with mean 0 and standard deviation σ. These distortions are tested with the proposed sleep algorithm as well as using the adversarial defenses discussed below.

3 Adversarial Defenses

We compare our sleep algorithm with two existing adversarial defenses: defensive distillation and fine-tuning, or adversarial retraining. Defensive distillation (Papernot et al. (2016b)) utilizes two training sessions in order to create a distilled network. First, an initial network is trained on (X, Y), where X is the training data, and Y is the one-hot encoded training labels. The activation function of this network is changed such that the softmax function of the output layer is computed using a temperature term T as follows:

$$F(x) = \frac{e^{\frac{z_i(X)}{T}}}{\sum_{l=0}^{N-1} e^{\frac{z_l(X)}{T}}}.$$

A higher value for T forces the ANN to produce probability values with large values for each class, whereas lower values for T support a similar representation as the one-hot encoded labels. After the first network is trained, the output of the network (probability values) is used to train a distilled network with the same softmax-temperature function. Previous work has shown this to be successful at preventing some types of attacks (Papernot et al. (2016b)). However, others have shown that it is not successful at defending against modified versions of those attacks or novel attacks in general (Carlini & Wagner (2016; 2017)). In our work, we use $T = 50$ to compare with the sleep algorithm.

Adversarial retraining aims to fine-tune the network on adversarial examples with the correct labels as a form of regularization. Previous work has shown that adversarial retraining can mitigate the effectiveness of some adversarial attacks. Goodfellow et al. (2014) showed that adversarial retraining can reduce the error rate on MNIST, demonstrating greater ANN robustness after fine-tuning. Likewise, Moosavi-Dezfooli et al. (2016) showed that fine-tuning on DeepFool attacks can reduce the effectiveness of their attacks. However, they observed that fine-tuning on FGSM attacks has negative results, actually increasing the strength of the attack. This suggests that fine-tuning may overfit the network to certain attacks, while failing to extrapolate to other attacks, similar to results shown for generalization in ANNs (Geirhos et al. (2018)). For the adversarial retraining procedure presented here, we train the network on the original input and then fine-tune the network on various adversarial attacks with a reduced learning rate.

4 SLEEP ALGORITHM

The basic intuition behind the sleep algorithm is that a period of offline activity, whereby network weights are modified according to an unsupervised learning algorithm, allows the parameters of the network to become more reflective of the underlying statistics of the task at hand, while not overfitting the statistics of the training data. The pseudocode is presented in Algorithm 1. In short, an ANN is trained using stochastic gradient descent and the usual backpropagation algorithm (exact parameters used for each of the datasets are shown in Table 1). After training, the network structure is converted into a spiking neural network (SNN). After building the SNN, we run a sleep phase which modifies the network connectivity based on spike-timing dependent plasticity (STDP). After the sleep phase, the SNN network is converted back into the ANN and testing is performed.

4.1 SPIKING NEURAL NETWORKS

While most ANNs are modelled after highly simplified brain dynamics, SNNs seek to more closely model temporal brain dynamics. In short, SNNs are composed of spiking neurons and model the information transformation and the dependence on exact timing of spikes that occurs in biological networks (Ghosh-Dastidar & Adeli (2009)). Neurons can range from simple integrate-and-fire type neurons which sum their inputs and produce an output (spike) if this exceeds some firing threshold to more complicated Hodgkin-Huxley type neurons which model sodium-, potassium-, and chloride-channel kinetics (Abbott & Kepler (1990)). Recent work has shown that a near loss-less conversion between ANNs and SNNs can be achieved by propagating activity through a spiking neural network for a given input and counting the number of times that each output neuron fires (Diehl et al. (2015)).

To convert an ANN to SNN (Lines 1-3 of pseudocode), we assume the ANN utilizes ReLU neurons with no bias. This assumption is made so that the output neuron's activation can be treated as a firing rate, either zero or positive, and that the thresholds of all neurons in a given layer are of the same scale. The weights from the ANN are directly mapped to the SNN. Each unit in the SNN is modelled as an integrate-and-fire type neuron, computing the following equation:

$$\tau_m \frac{dv}{dt} = -v(t) + \sum_{i=1}^{N} w_i * s(i).$$

Here, τ_m represents the decay constant of the membrane potential, v is the voltage at a given time, w_i is the weight connecting from neuron i, and $s(i)$ is the spiking activity of neuron i, either 1 or 0.

4.2 SLEEP

The key advantage of using a SNN is that biologically inspired training rules can be applied while the network is driven by noisy input. Empirical data suggest that the brain uses spike-timing dependent

Algorithm 1 Sleep:

procedure CONVERTANNTOSNN(nn)
  Map the weights from (nn) with ReLU units to network of integrate-fire units (snn)
  Apply weight normalization and return scale for each layer ([24]) **return** $snn, scales$
procedure CONVERTSNNTOANN(nn)
  Directly map the weights from integrate-fire network (nn) to ReLU network (ann) **return** ann
procedure SLEEP($nn, I, scales$) ▷ I is input
  Initialize v (voltage) $= 0$ vectors for all neurons
  for $t \leftarrow 1$ to Ts **do** ▷ Ts - duration of sleep
    $S(1) \leftarrow$ Convert input I to Poisson-distributed spike train
    for $l \leftarrow 2$ to n **do** ▷ n - number of layers
      $v(l,t) \leftarrow v(l,t-1) + (scales(l-1)\mathbf{W}(\mathbf{l},\mathbf{l-1})S(l-1))$ ▷ W(l,l-1) - weights
      $S(l) \leftarrow v(l,t) > threshold(l)$ ▷ Propagate spikes
      $\mathbf{W}(\mathbf{l},\mathbf{l-1}) \leftarrow \begin{cases} \mathbf{W}(\mathbf{l},\mathbf{l-1}) + inc & \text{if } S(l) = 1 \,\&\, S(l-1) = 1 \\ \mathbf{W}(\mathbf{l},\mathbf{l-1}) - dec & \text{if } S(l) = 1 \,\&\, S(l-1) = 0 \end{cases}$ ▷ STDP
procedure MAIN
  Initialize neural network (ann) with ReLU neurons and bias $= 0$.
  Train ann using backpropagation.
  $snn, scales$ = ConvertANNtoSNN(ann)
  snn = Sleep(snn, Training data X, $scales$)
  ann = ConvertSNNtoANN(snn)

plasticity (STDP) (Song et al., 2000), where weight updates depend on the relative timing of pre- and post-synaptic spikes. It has been shown that STDP results in balanced activity, where all neurons fire in equal proportions (Song et al. (2000)). Here we utilize a simplified version of STDP, resembling the classic Hebbian plasticity rule: if a pre-synaptic spike induces a post-synaptic spike, then the weight between these neurons is increased. If a post-synaptic spike occurs, but the pre-synaptic neuron does not spike, then the corresponding weight is decreased (in this case postsynaptic spiking may occur because of spiking in other neurons connecting to that post-synaptic neuron).

The sleep training phase we propose here can be described as following. First, inputs to each neuron of the input layer must be presented as spike-trains in order to propagate activity from the input layer to the hidden layers of the network. We convert inputs (real-valued pixel intensities or features) to spike trains by defining a maximum firing rate f_{max} with units $\frac{spikes}{sec}$ and computing a Poisson-distributed spike train, such that inputs with higher values (i.e. brighter pixels) will have higher rate than inputs with lower values, with no spike rates exceeding f_{max}. Next, activity is propagated through the network as spikes and the STDP rule is applied to update weights. To simulate sleep, with periods of up-states where activity is elevated and memory traces are thought to be replayed (resembling biological activity during deep sleep), weights are scaled by a parameter to induce high firing rates in later layers. Other important parameters include the threshold for each layer and the length of sleep. The parameters used for each dataset are presented in Table 2.

4.3 EXPERIMENTS AND DATASETS

Here, we describe the general experimental setup as well as the datasets tested. First, we trained a control ANN using the training set for each of the main datasets used in this study. Next, we created a defensively distilled network using $T = 50$ for the temperature parameter to create the second test network. Then, we fine-tuned the control ANN on a specific attack or distortion method to create the third test network. Finally, we converted the control ANN to an SNN and applied the sleep algorithm as described above to create the fourth test network. We created adversarial examples for each of these four networks using the attacks we described above (fine-tuned networks are tested on the attacks they were fine-tuned on). Then, we analyze how successful each attack is to fool each of the four networks using the metrics defined above. For generalization (blur and noise), we performed the same setup as above creating four different networks. We then tested each network on varying levels of distortion. We tested networks fine-tuned on blurred and noisy images to measure how

performance generalizes across distortion methods. We averaged performance across a minimum of three networks for each attack and distortion.

We used three datasets to compare performance: Patches (a toy dataset created simply for analysis), MNIST (LeCun et al. (1998)), and CUB-200 (Welinder et al. (2010)). Patches consists of four binary images arranged in a 10x10 square. Each image has its own label (1-4), and consists of 25 bright pixels (value set to 1) and 75 dark pixels. The overlap of bright pixels among the four images (see Appendix] Appendix) is chosen such that the task is not trivial. The MNIST dataset consists of 70,000 28x28 greyscale images of handwritten digits, with 60,000 in the training set and 10,000 in the testing set. CUB-200 is a high resolution dataset of images of birds with 200 bird species, with very few (30) images per class. For this dataset, we used previously extracted ResNet-50 embeddings, where ResNet-50 was pre-trained on ImageNet (He et al. (2016)). For CUB-200, we do not report results for blurring, since we are using extracted features, not images.

5 RESULTS

We evaluate the sleep algorithm in two settings: (1) Adversarial attacks designed to fool neural networks and (2) generalization distortions designed to reflect imperfect viewing conditions or other types of noise. For adversarial attacks (other than FGSM), we utilize the following metric to evaluate the success of each defense. Let x_i' be the adversarial example created for input x_i. The total score S_A for an attack is the median squared L2-distance for all samples, where N is the dimension of the space:

$$S_A = \textit{median}(\frac{1}{N} \|x_i' - x_i\|_2^2).$$

For FGSM, we define the following metric which computes the median minimum noise level η needed to produce a misclassification across all samples:

$$S_{FGSM} = \textit{median}(\textit{min}(\eta_i)) \textit{ s.t. } f(x_i + \eta_i * x_i') \neq f(x).$$

For MNIST and CUB-200, we evaluate the attacks on all examples in the testing set. Examples that the networks get wrong before the attack was implemented are discarded from the analysis (in these cases $\|x_i' - x\|_k^2 = 0$ and $\eta_i = 0$ for all attacks). For FGSM and distortions, we also include plots of accuracy as a function of noise level. For DeepFool and JSMA, we report adversarial attack accuracy (number of examples where $f(x) = y$ and $f(x') \neq f(x)$, where y is the correct label, over number of examples tested). Note that these algorithms would always produce an adversarial example if allowed to run forever. However, due to computational limitations, we included a run-time limitation on the number of iterations for these algorithms (see Appendix). Thus, a lower attack accuracy indicates that the attack would need more iterations to run to reach 100% accuracy. This is a similar measure as distance since more iterations would result in more distinct adversaries for all attacks implemented and the updates at each iteration have the same magnitude for each defense.

5.1 ADVERSARIAL ATTACKS

Patches	Control	Defensive Distillation	Fine-tuning	Sleep
FGSM	0.0175	0.05	0.1425	**0.2025**
DeepFool	**0.0440**(95.00%)	0.0360 **(90.00%)**	0.0201 (100.0%)	0.0124 (100.0%)
JSMA	0.0049 (80.00%)	0.0135 **(70.00%)**	0.0450 (100.0%)	**0.0541** (100.0%)
Boundary Attack	0.2971	0.3124	0.1772	**0.3515**

MNIST	Control	Defensive Distillation	Fine-tuning	Sleep
FGSM	0.0900	0.0900	0.1000	**0.2200**
DeepFool	0.0042 (96.46%)	0.0043 (96.42%)	0.0074 (97.40%)	**0.0484** **(86.38%)**
JSMA	0.0090 (99.29%)	**0.0086** (99.41%)	0.0133 (98.77%)	0.0059 **(72.97%)**
Boundary Attack	0.0525	0.0525	**0.0544**	0.0488

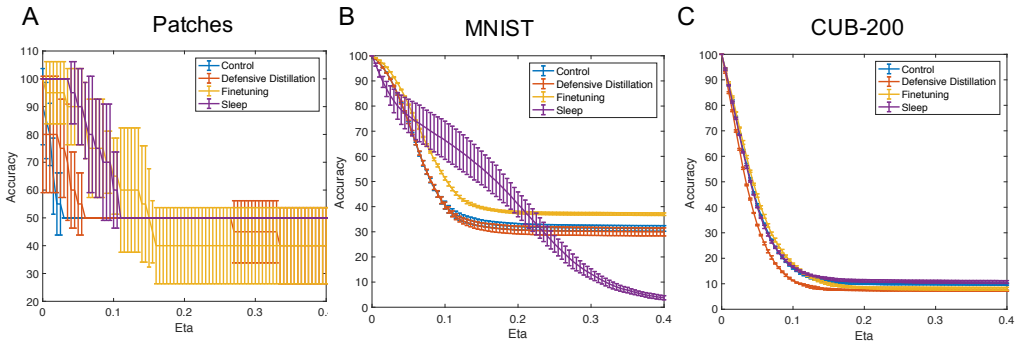

Figure 1: FGSM adversarial attack accuracy as a function of noise added (Eta) for the three datasets tested: A) Patches B) MNIST C) CUB-200.

CUB-200	Control	Defensive Distillation	Fine-tuning	Sleep
FGSM	0.0550	0.0500	**0.0650**	0.0600
DeepFool	0.0027 **(82.23%)**	0.0019 (84.16%)	**0.0044 (83.02%)**	0.0025 (83.12%)
JSMA	0.0477 (95.56%)	0.0347 (95.88%)	**0.0530** (95.38%)	0.0439 **(95.15%)**
Boundary Attack	0.9751	0.9034	**0.9976**	0.9967

Here we report the scores for all different attacks and for the all datasets. For the FGSM attack, the sleep algorithm increases the median minimum noise needed for misclassification for all three datasets compared to the control network (also see Figure 1). For MNIST dataset, the amount of noise needed to fool the network after the sleep algorithm was almost double of that needed for either the fine-tuning or defensive distillation approaches. For the Patches dataset, both defensive distillation and fine-tuning increase the robustness of the network. However, on CUB-200, only fine-tuning and sleep were able to defend, albeit marginally, against the FGSM attack. Looking at the accuracy of the network as a function of noise added (η, Figure 1), we observe that in the Patches and CUB-200 dataset, sleep has beneficial results in moving the accuracy function above the other defense methods. For MNIST, the baseline accuracy on the original test set decreases slightly compared to the other methods (80% after sleep). However, the performance remains high longer than for the other defense methods on images that were correctly classified. We observe that performance continued to drop after a sufficiently large amount of noise was added. This is biologically plausible as adding more noise to an image should result in misclassifications, as the images degrade. In sum, these results indicate that sleep phase can successfully mitigate FGSM, more so than a control network.

For DeepFool, sleep has a significant effect on the defense score on the MNIST dataset, both reducing the attack success rate and increasing the distance between the adversarial example and the original input by an order of magnitude. For Patches and CUB-200 this effect is less pronounced, with fine-tuning or the control network performing better. We hypothesize that sleep was ineffective in preventing the DeepFool attack in tasks with very few exemplars per class (Patches) or a large number of classes (CUB-200). In CUB-200, there is a large number of classes so the distance between the input and the nearest decision boundary is smaller (this is supported by the fact that JSMA, an L0 attack, does worse than DeepFool for CUB-200 and vice versa for MNIST, control networks). In this case, sleep is unable to move the decision boundary of one class without impinging on the decision space of another class. In MNIST, where the decision space for one class is presumably larger, sleep can alter decision boundaries in a way that has a minimal effect on other classes.

Sleep successfully increases the network's robustness to the JSMA atttacks for all three datasets, reducing the attack success rate in the case of CUB-200 and MNIST and increasing the distance needed to create an adversary for Patches. Defensive distillation and fine-tuning also reduce JSMA's effectiveness. However, for these two defenses, on MNIST and CUB-200 datasets, the networks were capable of finding an adversary for a higher percentage of the testing set. Thus, the effect of changing a small number of important pixels is mitigated after running sleep algorithm.

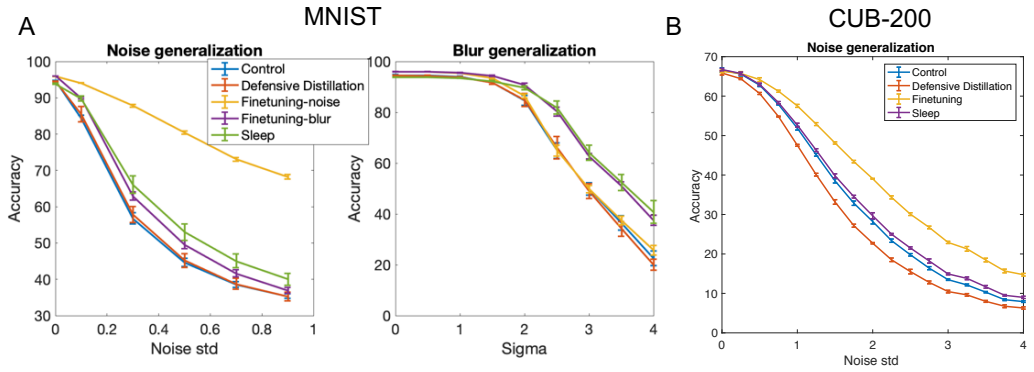

Figure 2: Generalization accuracy for noise and blur of five different networks tested (Control, Defensively distilled, Fine-tuned-blur, Fine-tuned-noise, and Sleep) for the following three datasets: A) MNIST B) CUB-200.

For the Boundary Attack, we found that no defense mechanism helps compared to the control in decreasing the attack's effectiveness on the MNIST dataset. However, for CUB-200 and Patches, the sleep algorithm results in a higher defense score than that for the control network. This lends support to the idea that sleep favorably alters decision boundaries so that it becomes harder to find an adversarial example that is close to the original image after the sleep phase. This also suggests that sleep is not simply obfuscating gradients, which has been a common criticism of several adversarial defenses (Athalye et al. (2018)), which are tested on white-box attacks. In fact, given the long run-time for convergence of this algorithm, if we define a threshold for adversarial attack success (L2-norm > 1), then sleep successfully defends against this attack on the MNIST dataset (see Table 3).

Why does sleep phase help? It has been shown that sleep tends to promote an increase in stronger weights while pruning weaker weights, thus increasing the width of the weights' distribution (Gonzalez et al., 2019). This results in the consolidation of strong memories at the cost of diminishing weak memories. From this point of view, a memory is a subspace or abstraction in the decision space corresponding to a given class. Sleep may result in enlarging the subspace the network allocates to a stronger category while shrinking weaker ones (Figure 8A). The process of strengthening the strong memory also results in making it robust and noise invariant, as seen in Figure 8B where the first 8 categories (numbers 0-7) are strengthened and become more invariant to the FGSM attack, while the last two digits are essentially forgotten and the network cannot confidently predict exemplars from these classes (Figure 8C). If the noise is less targeted, as in the case of random noise or blurring, sleep does not need to alter the decision space as much to produce better generalization and can maintain a high baseline accuracy, as we demonstrate in the next section.

5.2 Generalization

Figure 2 shows the network performance for noisy and blurry distortions of data for MNIST (A) as well as noisy distortions for the CUB-200 feature embeddings (B, see Figure 5 for results on Patches). Overall, fine-tuning on an image distortion results in the best performance for that specific distortion. However, as was noted (Geirhos et al. (2018)), fine-tuning on a specific distortion does not extend to other types of distortions. In our analysis, fine-tuning the network on blurred MNIST images results in high performance ($> 80\%$) on blurred images. However, for noisy images, this performance was only marginally above the control network. The sleep algorithm increased performance for both distortion methods, since this approach is not tailored to any one representation of the training set.

Finally we tested how sleep increases robustness on blur and noise distortions. In biological systems, sleep increases generalization through replay of memories learned during awake which leads to changes in synaptic weights. These changes entail both an increase in synaptic weights associated with a specific task and pruning of synapses involved in other tasks (Gonzalez et al., 2019; Tononi & Cirelli, 2006). Figures 14 and 15 show that correlations among like digits in the hidden layers

of the network are greater after applying sleep than before for noisy and blurred images. Likewise, pairs of different digits usually become decorrelated after sleep, suggesting synaptic pruning. We also show that both normalized spiking activity and activations of digit-specific neurons are higher after sleep than before (Figures 16 and 17, see Appendix for details). These results suggest that the sleep algorithm increases robustness through biologically plausible learning mechanisms involving replay of relevant activity during sleep phase.

6 Conclusions and Future Directions

In this work, we show that a biologically inspired sleep algorithm can increase an ANN's robustness to both adversarial attacks and general image distortions. The algorithm augments the normal (e.g., back-propagation based) training phase of an ANN with an unsupervised learning phase in the equivalent SNN modelled after how the biological brain learns using Hebbian type plasticity rules. We hypothesize that the unsupervised sleep phase creates more natural feature representations which in turn lead to more natural decision boundaries, thus increasing the robustness of the network. Although this robustness may come at a cost of overall accuracy, it has been shown that robustness may have multiple important benefits, such as more salient feature representations as well as invariance to input modifications (Tsipras et al. (2018)). We also show that the trade-off between robustness and accuracy does not always occur, particularly for image distortions such as noise or blur. Future work includes converting the sleep algorithm into a regularization technique to be applied in more standardized machine learning frameworks as well as understanding the theoretical basis for the beneficial role of spike based plasticity rules in increasing network robustness.

References

LF Abbott and Thomas B Kepler. Model neurons: from hodgkin-huxley to hopfield. In *Statistical mechanics of neural networks*, pp. 5–18. Springer, 1990.

Anish Athalye, Logan Engstrom, Andrew Ilyas, and Kevin Kwok. Synthesizing robust adversarial examples. *arXiv preprint arXiv:1707.07397*, 2017.

Anish Athalye, Nicholas Carlini, and David Wagner. Obfuscated gradients give a false sense of security: Circumventing defenses to adversarial examples. *arXiv preprint arXiv:1802.00420*, 2018.

Battista Biggio and Fabio Roli. Wild patterns: Ten years after the rise of adversarial machine learning. *Pattern Recognition*, 84:317–331, 2018.

Wieland Brendel, Jonas Rauber, and Matthias Bethge. Decision-based adversarial attacks: Reliable attacks against black-box machine learning models. *arXiv preprint arXiv:1712.04248*, 2017.

Nicholas Carlini and David Wagner. Defensive distillation is not robust to adversarial examples. *arXiv preprint arXiv:1607.04311*, 2016.

Nicholas Carlini and David Wagner. Towards evaluating the robustness of neural networks. In *2017 IEEE Symposium on Security and Privacy (SP)*, pp. 39–57. IEEE, 2017.

Peter U Diehl, Daniel Neil, Jonathan Binas, Matthew Cook, Shih-Chii Liu, and Michael Pfeiffer. Fast-classifying, high-accuracy spiking deep networks through weight and threshold balancing. In *2015 International Joint Conference on Neural Networks (IJCNN)*, pp. 1–8. IEEE, 2015.

Samuel Dodge and Lina Karam. Understanding how image quality affects deep neural networks. In *2016 eighth international conference on quality of multimedia experience (QoMEX)*, pp. 1–6. IEEE, 2016.

Nic Ford, Justin Gilmer, Nicolas Carlini, and Dogus Cubuk. Adversarial examples are a natural consequence of test error in noise. *arXiv preprint arXiv:1901.10513*, 2019.

Robert Geirhos, Carlos RM Temme, Jonas Rauber, Heiko H Schütt, Matthias Bethge, and Felix A Wichmann. Generalisation in humans and deep neural networks. In *Advances in Neural Information Processing Systems*, pp. 7538–7550, 2018.

Samanwoy Ghosh-Dastidar and Hojjat Adeli. Spiking neural networks. *International journal of neural systems*, 19(04):295–308, 2009.

Oscar C Gonzalez, Yury Sokolov, Giri Krishnan, and Maxim Bazhenov. Can sleep protect memories from catastrophic forgetting? *BioRxiv*, pp. 569038, 2019.

Ian J Goodfellow, Jonathon Shlens, and Christian Szegedy. Explaining and harnessing adversarial examples. *arXiv preprint arXiv:1412.6572*, 2014.

Kaiming He, Xiangyu Zhang, Shaoqing Ren, and Jian Sun. Deep residual learning for image recognition. In *Proceedings of the IEEE conference on computer vision and pattern recognition*, pp. 770–778, 2016.

Ruitong Huang, Bing Xu, Dale Schuurmans, and Csaba Szepesvari. Learning with a strong adversary. *arXiv preprint arXiv:1511.03034*, 2015.

Alex Krizhevsky, Ilya Sutskever, and Geoffrey E Hinton. Imagenet classification with deep convolutional neural networks. In *Advances in neural information processing systems*, pp. 1097–1105, 2012.

Yann LeCun, Léon Bottou, Yoshua Bengio, Patrick Haffner, et al. Gradient-based learning applied to document recognition. *Proceedings of the IEEE*, 86(11):2278–2324, 1998.

Penelope A Lewis and Simon J Durrant. Overlapping memory replay during sleep builds cognitive schemata. *Trends in cognitive sciences*, 15(8):343–351, 2011.

Seyed-Mohsen Moosavi-Dezfooli, Alhussein Fawzi, and Pascal Frossard. Deepfool: a simple and accurate method to fool deep neural networks. In *Proceedings of the IEEE conference on computer vision and pattern recognition*, pp. 2574–2582, 2016.

Anh Nguyen, Jason Yosinski, and Jeff Clune. Deep neural networks are easily fooled: High confidence predictions for unrecognizable images. In *Proceedings of the IEEE conference on computer vision and pattern recognition*, pp. 427–436, 2015.

Nicolas Papernot, Patrick McDaniel, Somesh Jha, Matt Fredrikson, Z Berkay Celik, and Ananthram Swami. The limitations of deep learning in adversarial settings. In *2016 IEEE European Symposium on Security and Privacy (EuroS&P)*, pp. 372–387. IEEE, 2016a.

Nicolas Papernot, Patrick McDaniel, Xi Wu, Somesh Jha, and Ananthram Swami. Distillation as a defense to adversarial perturbations against deep neural networks. In *2016 IEEE Symposium on Security and Privacy (SP)*, pp. 582–597. IEEE, 2016b.

Jessica D Payne, Daniel L Schacter, Ruth E Propper, Li-Wen Huang, Erin J Wamsley, Matthew A Tucker, Matthew P Walker, and Robert Stickgold. The role of sleep in false memory formation. *Neurobiology of learning and memory*, 92(3):327–334, 2009.

Björn Rasch and Jan Born. About sleep's role in memory. *Physiological reviews*, 93(2):681–766, 2013.

Jonas Rauber, Wieland Brendel, and Matthias Bethge. Foolbox: A python toolbox to benchmark the robustness of machine learning models. *arXiv preprint arXiv:1707.04131*, 2017.

David Silver, Aja Huang, Chris J Maddison, Arthur Guez, Laurent Sifre, George Van Den Driessche, Julian Schrittwieser, Ioannis Antonoglou, Veda Panneershelvam, Marc Lanctot, et al. Mastering the game of go with deep neural networks and tree search. *nature*, 529(7587):484, 2016.

Sen Song, Kenneth D Miller, and Larry F Abbott. Competitive hebbian learning through spike-timing-dependent synaptic plasticity. *Nature neuroscience*, 3(9):919, 2000.

Robert Stickgold. Sleep-dependent memory consolidation. *Nature*, 437(7063):1272, 2005.

Robert Stickgold and Matthew P Walker. Sleep-dependent memory triage: evolving generalization through selective processing. *Nature neuroscience*, 16(2):139, 2013.

Christian Szegedy, Wojciech Zaremba, Ilya Sutskever, Joan Bruna, Dumitru Erhan, Ian Goodfellow, and Rob Fergus. Intriguing properties of neural networks. *arXiv preprint arXiv:1312.6199*, 2013.

Giulio Tononi and Chiara Cirelli. Sleep function and synaptic homeostasis. *Sleep medicine reviews*, 10(1):49–62, 2006.

Dimitris Tsipras, Shibani Santurkar, Logan Engstrom, Alexander Turner, and Aleksander Madry. Robustness may be at odds with accuracy. *arXiv preprint arXiv:1805.12152*, 2018.

Jonathan Uesato, Brendan O'Donoghue, Aaron van den Oord, and Pushmeet Kohli. Adversarial risk and the dangers of evaluating against weak attacks. *arXiv preprint arXiv:1802.05666*, 2018.

Igor Vasiljevic, Ayan Chakrabarti, and Gregory Shakhnarovich. Examining the impact of blur on recognition by convolutional networks. *arXiv preprint arXiv:1611.05760*, 2016.

Erin J Wamsley, Matthew A Tucker, Jessica D Payne, and Robert Stickgold. A brief nap is beneficial for human route-learning: The role of navigation experience and eeg spectral power. *Learning & Memory*, 17(7):332–336, 2010.

Yina Wei, Giri P Krishnan, Maxim Komarov, and Maxim Bazhenov. Differential roles of sleep spindles and sleep slow oscillations in memory consolidation. *PLoS computational biology*, 14 (7):e1006322, 2018.

Peter Welinder, Steve Branson, Takeshi Mita, Catherine Wah, Florian Schroff, Serge Belongie, and Pietro Perona. Caltech-ucsd birds 200. 2010.

Matthew A Wilson and Bruce L McNaughton. Reactivation of hippocampal ensemble memories during sleep. *Science*, 265(5172):676–679, 1994.

Xiaoyong Yuan, Pan He, Qile Zhu, and Xiaolin Li. Adversarial examples: Attacks and defenses for deep learning. *IEEE transactions on neural networks and learning systems*, 2019.

Yiren Zhou, Sibo Song, and Ngai-Man Cheung. On classification of distorted images with deep convolutional neural networks. In *2017 IEEE International Conference on Acoustics, Speech and Signal Processing (ICASSP)*, pp. 1213–1217. IEEE, 2017.

7 Appendix

7.1 Training Parameters

Here, we define the neural network parameters used for each of the three datasets as well as the sleep, defensive distillation, and fine-tuning parameters used. Table 1 shows the neural network training parameters used to train each of the control networks discussed in the paper. All neural networks were trained with ReLU neurons. Table 2 shows the parameters used during sleep on each of the three datasets. Note that these parameters (for MNIST and CUB-200) were chosen by running a genetic algorithm to maximimize performance on the FGSM attack (performance was determined based on the training set so as not to overfit to the test set). For the other three attacks, parameters that maximized FGSM performance were used. Also, for noise and blur generalization, different parameters were chosen (not shown here).

	Patches	MNIST	CUB200
Architecture	[100, 4]	[784, 1200, 1200, 10]	[2048, 350, 300, 200]
Learning Rate	0.1	0.1	0.1
Momentum	0.5	0.5	0.5
Dropout	0	0.2	0.25
Epochs	1	2	100

Table 1: Parameters used to train the control network for each of the three datasets. Architecture refers to number of units per layer. For example, the MNIST network possessed 1 input layer, 2 hidden layers with 1200 units, and an output unit with 10 units.

	Patches	MNIST	CUB200
Input Rate	16 Hz	40 Hz	79 Hz
Sleep Duration	3000	27105	11751
Thresholds	1.0450, 0.7150, 0.3850	36.18, 23.36, 36.38	2.69, 4.61, 2.63
Synaptic AMPA current	4.25	2.19	4.15
Increase factor	0.0035	0.063	0.0016
Decrease factor	0.0002	0.069	0.000209

Table 2: Parameters used during sleep. Input rate = F_{max}, the maximum firing rate of input neurons, Sleep duration = length of sleep (number of images presented during sleep, Thresholds = neuronal firing thresholds for each layer of neurons, Synaptic AMPA current = factor to scale the weights by during sleep, Increase and Decrease factor = amount weights are modified on a STDP event.

For the defensively distilled networks tested in the paper, we first train an initial network using a temperature of 50. Then, we use the training set to compute soft labels and finetune the initial network on these soft labels for the same number of epochs and with the same learning rate.

For the fine-tuned networks, we take the control networks trained with the parameters shown in Table 1. The learning rate is reduced to 0.05 and the network is fine-tuned on a mixture of either adversarial attacks, blur or noise and the original images/features. For CUB-200, we perform fine-tuning for 10 epochs.

7.2 Patches Analysis

The Patches dataset represents an easily interpretable example where we can understand what happens to the weights after sleep. Figure 3 shows an example of the dataset. Here, we have 4 images each belonging to 4 different classes. 25 pixels are whitened in each image and the remaining 75 pixels are dark. There is a 15 pixel overlap, so that weights connecting from input to output layer must take this into account in order to separate the images. Figure 4 illustrate the blur and noise distortions tested for this dataset and Figure 5 shows the results for the blur and noise distortions.

After the network is trained, we can analyze the weights connecting from each of the 100 input neurons to the 4 output neurons (see Figure 6, top row). We theorize that optimally robust behavior would occur when weights connecting from ON-pixels are positive, weights connecting from overlapping pixels are near 0, and weights connecting from OFF-pixels are negative. In this case, changing the value of overlapping pixels will have no effect on classification. Changing the value of OFF-pixels will cause the network to predict another class, where OFF-pixels may be ON-pixels or indicative of that class. Changing the value of ON-pixels will only have a negative impact if the brightness of the pixel is reduced significantly. Thus, in this circumstance, the network should behave robustly.

In the control network, we observe that weights connecting from ON-pixels (pixel-value = 1) increase while weights connecting from OFF-pixels remain at 0. Weights connecting from overlapping pixels remain near 0 or positive. Defensive distillation causes some weights connecting from overlapping pixels to decrease, likely because the soft labels used in defensive distillation cause overlapping pixel units to alter the probability values computed by the network in such a way that does not truly reflect the impact of the overlapping pixels. In the fine-tuning networks (both on blurred images and noisy images), we observe an increase in ON-pixel weights and an increase in noisiness of OFF-pixel weights. Likewise, in the sleep network, OFF-pixel weights become negative while ON-pixel weights remain the same. In these cases, robustness is increased as weights become more similar to our hypothesized ideal weights. Essentially, the magnitude of input changes need to change classification increase since the spread between ON-pixel weights and OFF-pixel weights increases. We quantify the spread in weights by taking the difference between the average weight connecting from ON-pixels and the average weight connecting from OFF-pixels. This represents the mean input that each correct output neuron receives. This result is shown in Figure 7. Of note is that this weight spread is increased for both the sleep and finetuning-noise network, suggesting that these defenses bring the weights closer to their ideal values for computing robustness.

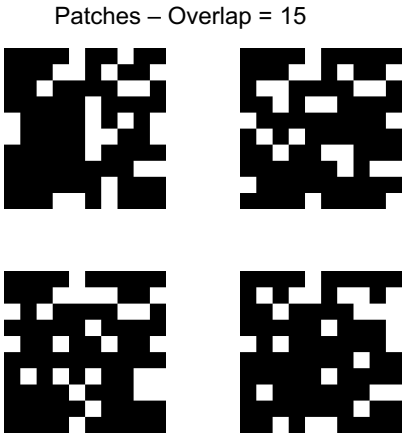

Figure 3: Patches dataset example

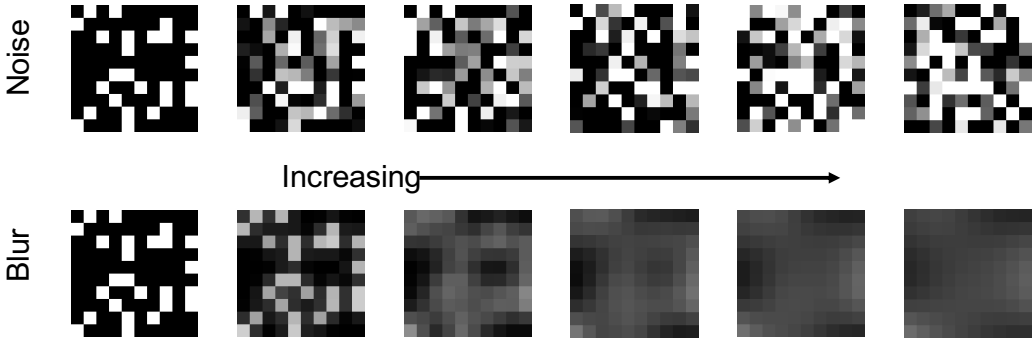

Figure 4: Types of images tested on for generalization for the Patches dataset. Top - Images with Gaussian noise added with increasing variannce (from 0 to 1.0 in steps of 0.2). Bottom - Gaussian blurred images with increasing sigma (from 0 to 2.5 in steps of 0.5).

7.3 Adversarial Attacks

Here, we describe the general approach for implementing DeepFool, JSMA, and the Boundary Attack discussed in the paper. We also show examples of adversaries created for each of the defense networks from these attacks.

DeepFool. DeepFool (Moosavi-Dezfooli et al. (2016)), as mentioned above, is an iterative algorithm that, at each iteration, aims to move the adversarial example in the direction of the closest decision boundary until it results in a misclassification. We based our implementation off of that in Rauber et al. (2017). We stopped running the algorithm when either an adversarial example is found or when 100 iterations have passed. Examples of DeepFool attacks on the MNIST dataset are shown in Figure 9. At each iteration we compute a linear approximation of the loss function and take a step in the direction that would be result in a misclassification. The equations used and pseudocode can be found in the original DeepFool paper.

JSMA. JSMA is also an iterative algorithm which computes the pixel that would change the loss function the most at each algorithm and changes this pixel, until a misclassification is produced. For this method, we set a run-time limit of 500 iterations. We also remove a pixel from the saliency map when it has beeen updated seven times, so the algorithm can focus on other pixels. We set the

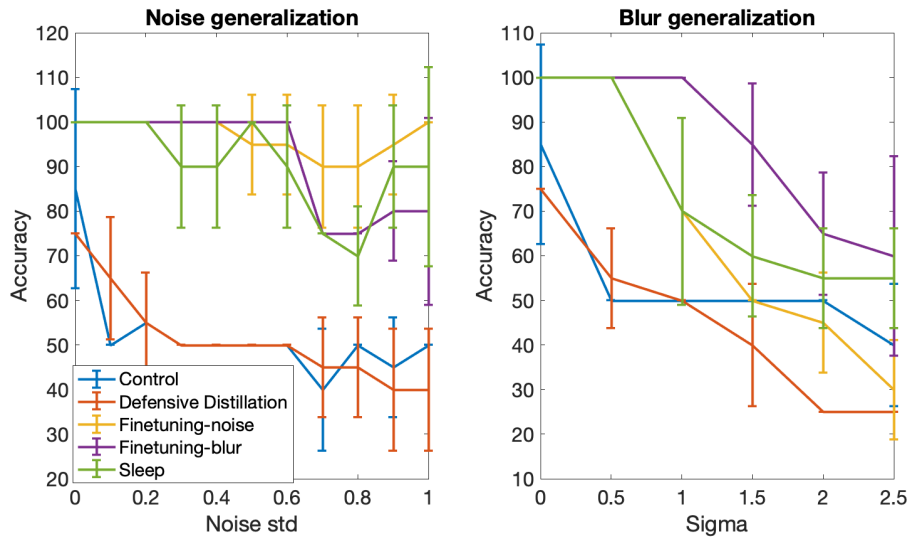

Figure 5: Generalization accuracy for noise and blur of five different networks tested (Control, Defensively distilled, Fine-tuned-blur, Fine-tuned-noise, and Sleep) for the Patches dataset.

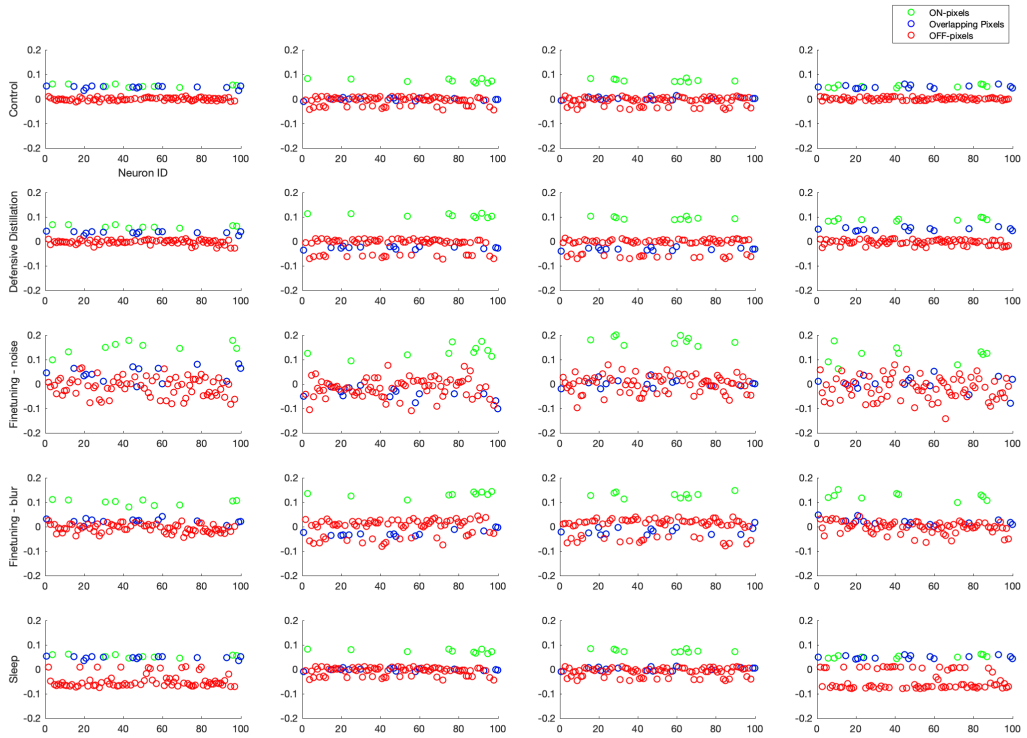

Figure 6: Weights for each of the 5 networks (Control, defensively distilled, finetuning on noise, finetuning on blur, and sleep) trained on Patches dataset. Each column shows the weights connecting from each of the 100 input neurons (x-axis) to the corresponding output neuron.

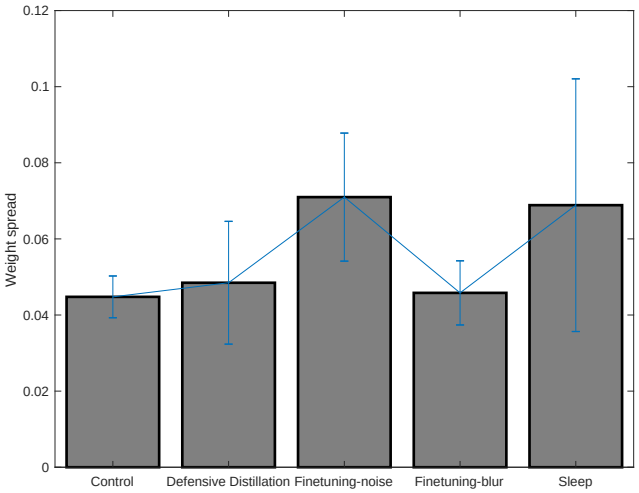

Figure 7: Weight spread for each of the 5 networks.

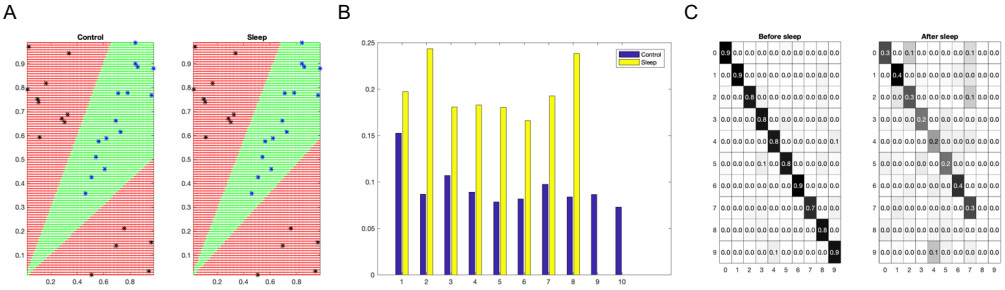

Figure 8: A) Example function learned in a 3-layer neural network illustrates that sleep alters decision boundaries in favor of making one class more robust while impinging on another class. B) Average noise needed for FGSM attack for specific digits. C) Output layer scores for each digit (rows) before and after sleep.

MNIST	Control	Defensive Distillation	Fine-tuning	Sleep
Boundary Attack	0.0073	0.0074	0.0047	**0.0094**

Table 3: MNIST Boundary Attack with a threshold defining a successful adversarial attack.

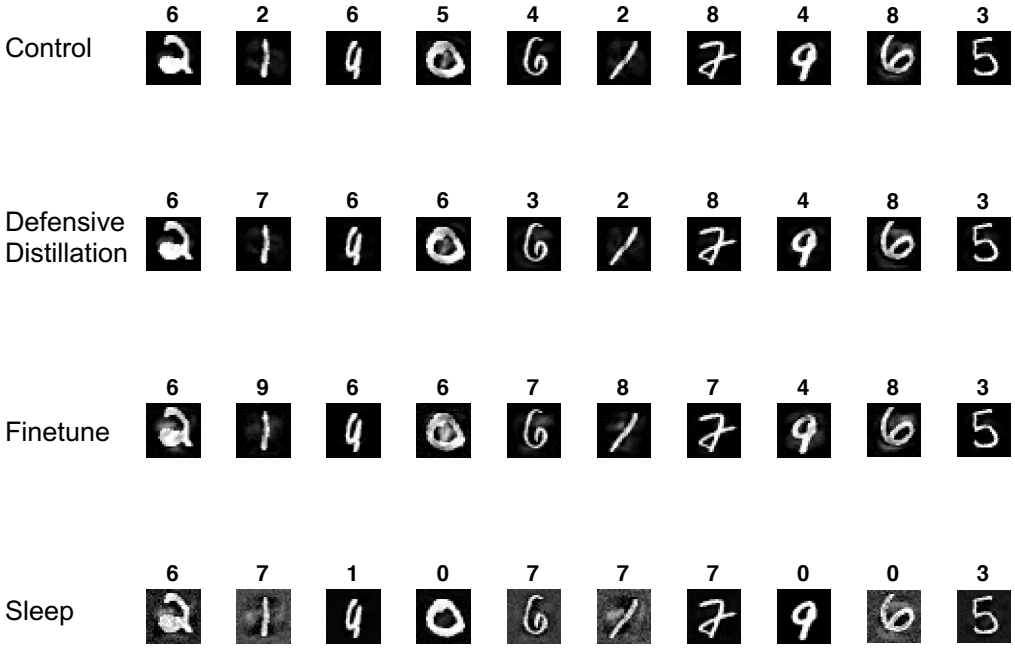

Figure 9: DeepFool adversarial examples for each defense. The network's prediction is shown above each image.

change to each pixel at a constant value, 0.1. This represents how much each pixel is updated (in the direction that results in a misclassification) at each iteration. Pseudocode can be found in the original publication (Papernot et al. (2016a)). We show examples of adversaries created by JSMA in Figure 10.

Boundary Attack. The Boundary Attack (Brendel et al. (2017)) starts with an adversarial example and moves it closer to the decision boundary of the correct class. At each step of the algorithm, the method performs orthogonal and forward perturbations to move the adversary closer to the original image, thus reducing the distance between the adversary and the original image. We set both a distance convergence criterion (L2-norm = 1e-7) and a run-time limitation on the attack (1000 iterations). Example attacks are shown in Figure 11. We note that sometimes the algorithm does not successfully produce an "imperceptible" adversarial example and instead produces a noisy output (the starting condition is a noisy image). If we define a threshold defining a successful adversarial attack (L2-Norm > 1), then we observe the results for MNIST in Table 3.

7.4 Generalization Analysis

In this section, we analyze how sleep can aid in increasing ANN robustness. In biological networks, sleep extracts the gist of a task through replay (Lewis & Durrant (2011)). Thus, we hypothesized that our sleep algorithm works in the same manner. First, we tested the ability of the sleep network to decorrelate distinct inputs. We tested this hypothesis by analyzing the effect of running sleep and testing on our two distortion techniques (see Figure 12).

First, we computed the correlations of network activities in each of the hidden layers of the network before and after implementing our defense methods. For each pair of digits, we computed the

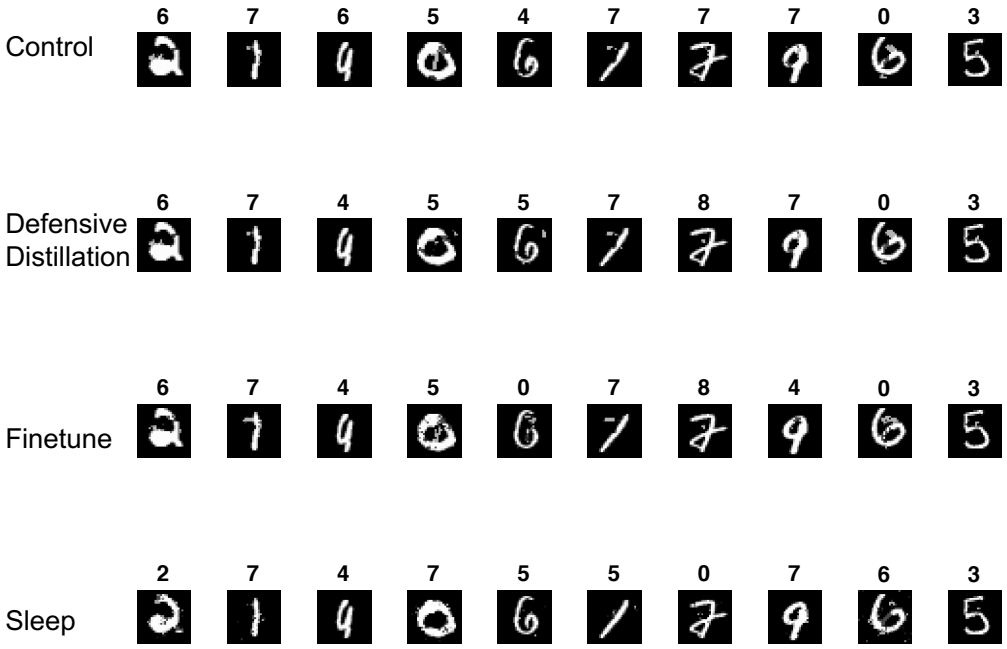

Figure 10: JSMA adversarial examples for each defense. The network's prediction is shown above each image.

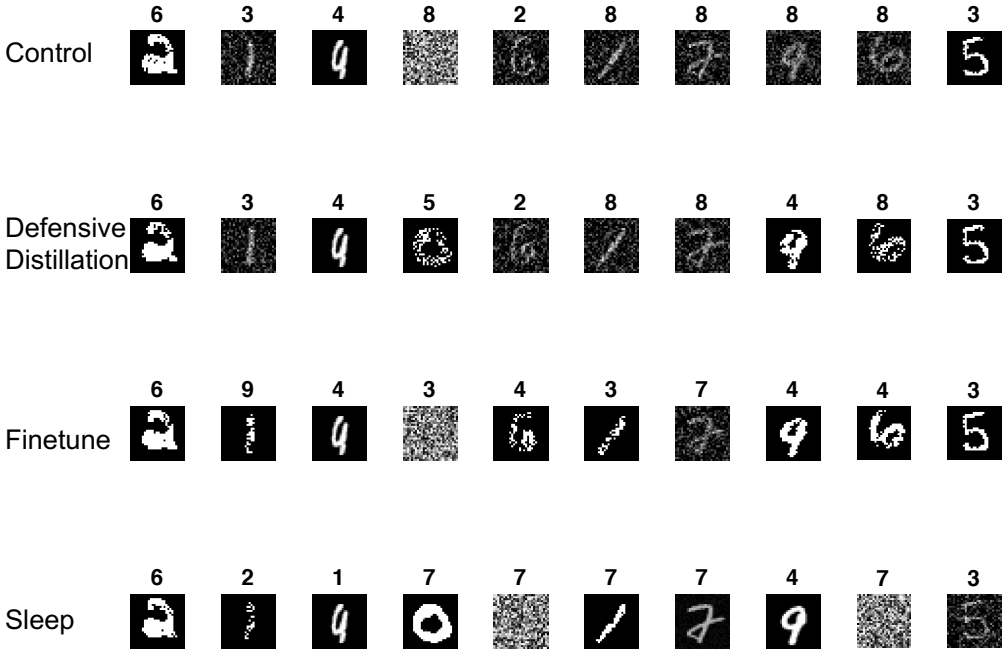

Figure 11: Boundary Attack adversarial examples for each defense. The network's prediction is shown above each image.

average correlation of layer activities in the undistorted (Figure 13), noisy (Figure 14), and blurred (Figure 15) conditions. Each figure reports the difference in digit pairwise correlations between the defense method and the control network for each set of inputs. For our sleep network, it is apparent that in layer 2 and layer 3, the correlations of the same digits (the diagonal) increases after sleep. Additionally, the correlation of distinct digits typically experiences negative change, representing decorrelation of distinct inputs. This analysis holds for defensive distillation and both of the fine-tuned networks. This suggests that the ANN representation of different exemplars of the same digit becomes more similar after sleep or after any of the defense networks when compared to the control. This is not simply due to an increased overlap of all inputs, since exemplars of different digits become decorrelated after applying a defense method.

Next, we performed the same correlation analysis on noisy and blurred images to see how the representation of distorted images changes after applying a distortion method. First, we note that fine-tuning on noisy images results in stronger correlation of the same (noisy) digit but weaker correlations of different (noisy) digits, as noted above. However, fine-tuning on blurred images does not have as strong an effect. Second, sleep seems to have a beneficial effect on the correlation matrices for both blurred and noisy images (comparing the right column of Figures 14 and 15). This illustrates the beneficial role of sleep in creating distinct representations of digits, where different neuronal ensembles encode different digits. This change in representation should result in increased robustness since changes to the input must be larger in order to recruit neuronal ensembles that represent other digits.

On top of decorrelating the representation of distinct memories by pruning synapses, biophysical modelling suggests that sleep can also aid in strengthening connections thus making the response of primary neurons involved in memory much stronger (Gonzalez et al. (2019)). To test this hypothesis in our networks, we analyzed the firing rate and activations of digit-specific neurons before and after sleep. Before describing the analysis, we remind the reader that SNNs can be used to performn classification and a near loss-less conversion between ANNs and SNNs has been achieved on the MNIST task (Diehl et al. (2015)). To perform classification, a digit is presented (as a Poisson spike train) to the network and spikes are propagated throughout the network for a given time period (or number of presentations of the input). Analyzing network activity in the spiking domain can be easier than in the activation domain (ANNs) since spikes are oftentimes easier to interpret than neuronal activations.

For this reason, we first analyze how spike rates of digit-specific neurons change before and after sleep in the spike domain. To do this we present all images of a specified digit to the spiking network and count the number of spikes from each neuron (holding the weights constant). We define digit-specificity by looking at the 100 neurons with the highest firing rates in layer 2. In Figure 16, we show that the normalized firing rate of these neurons usually increases after sleep (normalized by dividing by the maximum firing rate observed from the SNN).

Next, we perform the same analysis in the activation domain. Again, we define digit-specific neurons by looking at the top 100 neurons with the highest activation for a specific digit. We look at the normalized mean activations of these neurons before and after sleep and note that for all digits this value is higher after sleep than before sleep (Figure 17). This suggests that the neurons in the network are responding more strongly to the presentation of the same digit, thus increasing the robustness of the network as more noise must be added in order to counter the effect of this stronger response. This also suggests that our algorithm works in a biologically plausible way: both by decorrelating distinct inputs and increasing the strength of similar inputs.

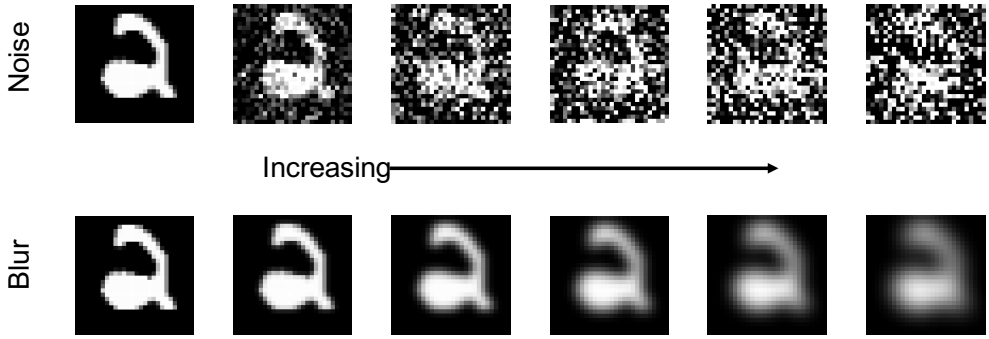

Figure 12: Types of images tested on for generalization for the MNIST dataset. Top - Images with Gaussian noise added with increasing variannce (0, 0.1, 0.3, 0.5, 0.7, 0.9, left to right). Bottom - Gaussian blurred images with increasing sigma (from 0 to 2.5 in steps of 0.5).

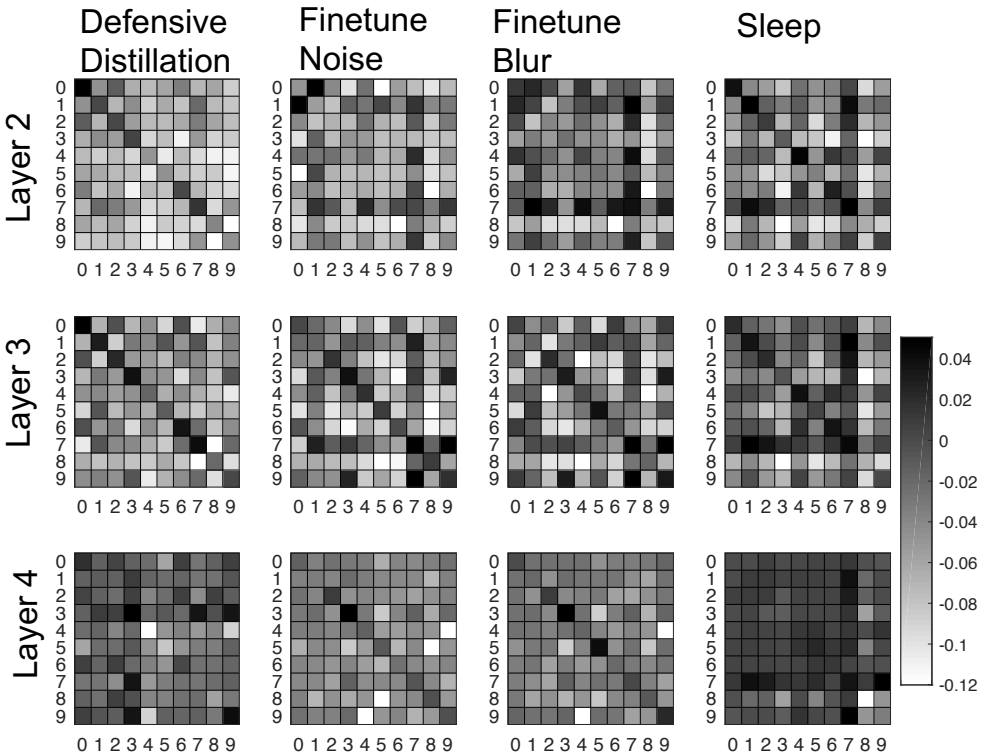

Figure 13: Correlation differences between defense network and control network for 4 different defenses. Correlations are computed based on the activations in each layer for each pair of digits (mean correlation). The difference between the correlation of the defense method (column) and the control network is plotted. Activations are computed based on the undistorted test images.

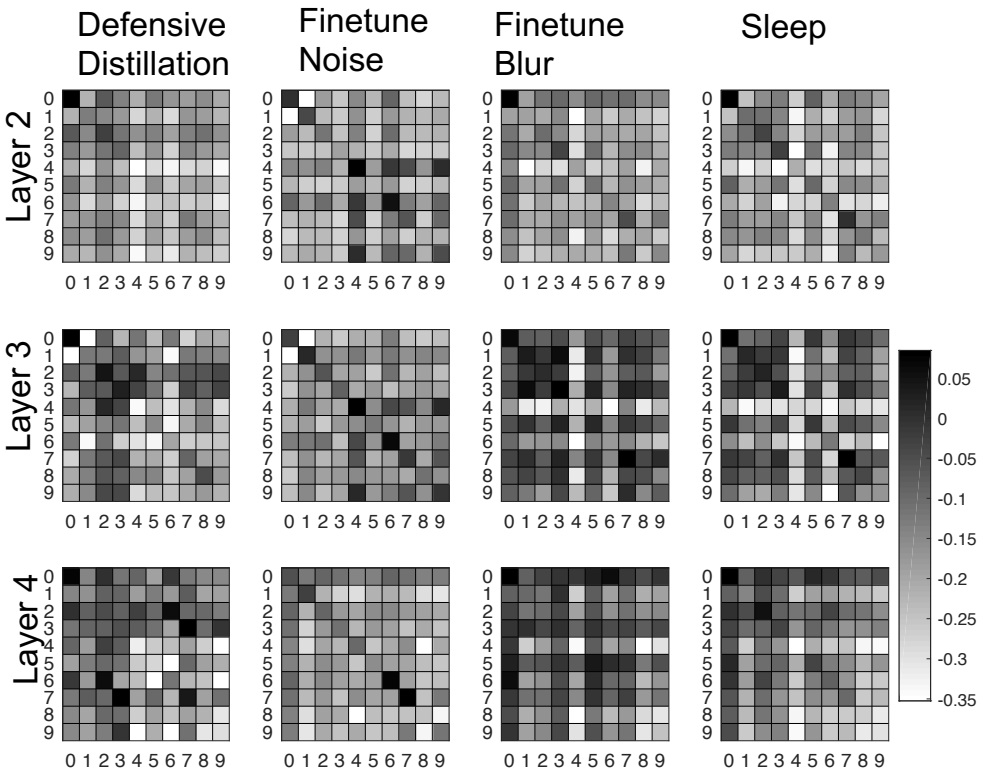

Figure 14: same as Figure 13 but activations are computed when presented with noisy images.

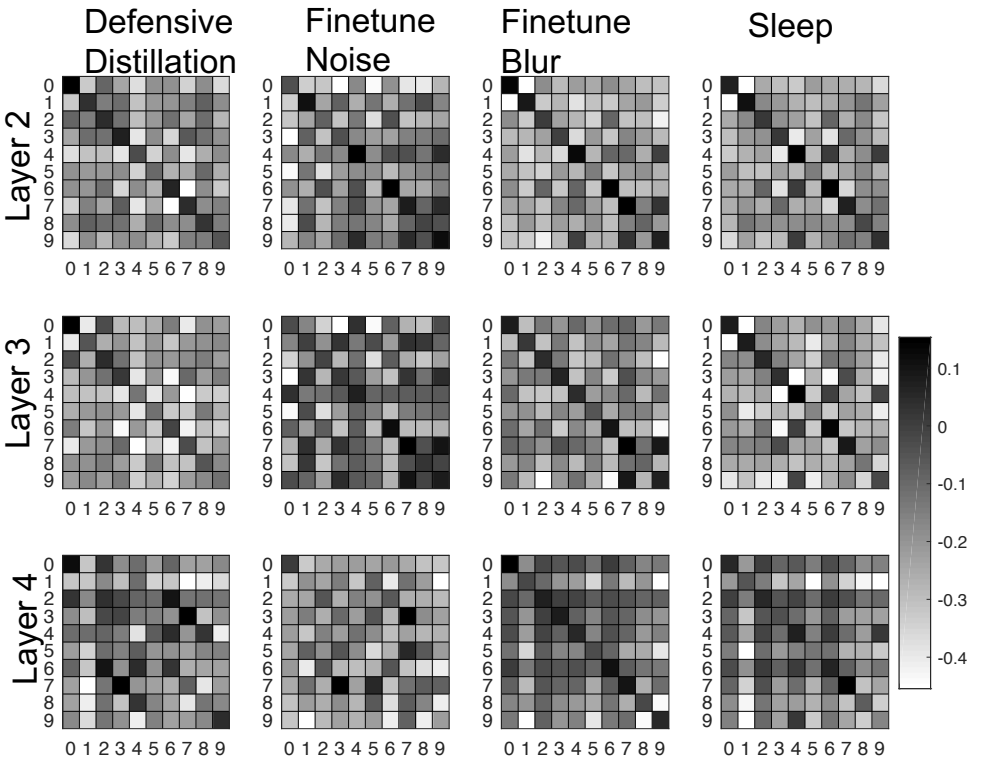

Figure 15: same as Figure 13 but activations are computed when presented with blurred images.

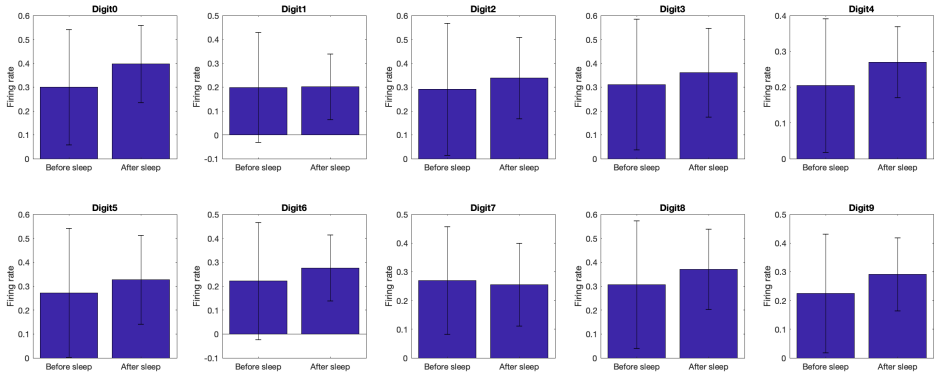

Figure 16: Normalized firing rates of neurons specific to individual digits when presented with noisy images is greater after applying sleep than before sleep.

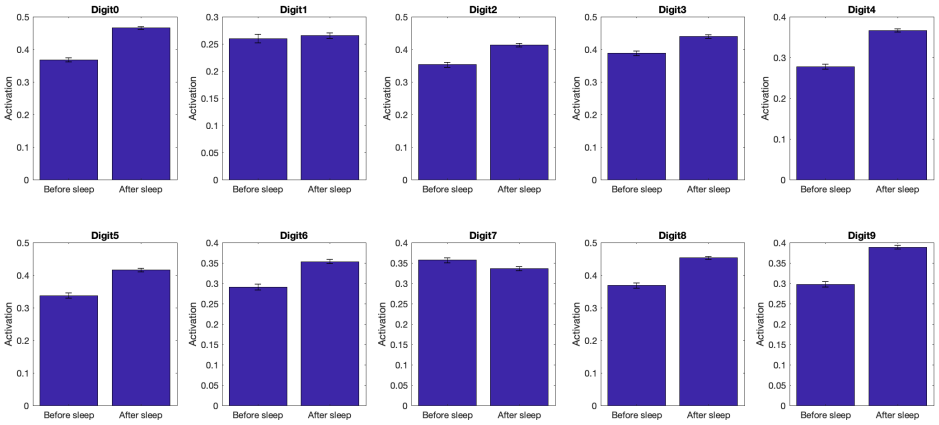

Figure 17: Normalized activations of neurons specific to individual digits when presented with noisy images is greater after applying sleep than before sleep.